

Open form of syntaxin-1A is a more potent inhibitor than wild-type syntaxin-1A of Kv2.1 channels

Yuk M. LEUNG, Youhou KANG, Fuzhen XIA, Laura SHEU, Xiaodong GAO, Huanli XIE, Robert G. TSUSHIMA¹ and Herbert Y. GAISANO¹

Departments of Medicine and Physiology, University of Toronto, Toronto, Canada M5S 1A8

We have shown that SNARE (soluble *N*-ethylmaleimide-sensitive fusion protein attachment protein receptor) proteins not only participate directly in exocytosis, but also regulate the dominant membrane-repolarizing Kv channels (voltage-gated K⁺ channels), such as Kv2.1, in pancreatic β -cells. In a recent report, we demonstrated that WT (wild-type) Syn-1A (syntaxin-1A) inhibits Kv2.1 channel trafficking and gating through binding to the cytoplasmic C-terminus of Kv2.1. During β -cell exocytosis, Syn-1A converts from a closed form into an open form which reveals its active H3 domain to bind its SNARE partners SNAP-25 (synaptosome-associated protein of 25 kDa) and synaptobrevin. In the present study, we compared the effects of the WT Syn-1A and a mutant open form Syn-1A (L165A, E166A) on Kv2.1 channel trafficking and gating. When co-expressed in HEK-293 cells (human embryonic kidney-293 cells), the open form Syn-1A decreased Kv2.1 current density more than ($P < 0.05$) the WT Syn-1A (166 ± 35 and 371 ± 93 pA/pF respectively; control = 911 ± 91 pA/pF). Confocal microscopy and biotinylation experiments showed that both the WT and open form Syn-1A inhibited Kv2.1 expression at the plasma membrane to a similar extent, suggesting that the stronger reduction of Kv2.1 current density by the open form compared with the WT Syn-1A is probably

due to a stronger direct inhibition of channel activity. Consistently, dialysis of the recombinant open form Syn-1A protein into Kv2.1-expressing HEK-293 cells caused stronger inhibition of Kv2.1 current amplitude ($P < 0.05$) than the WT Syn-1A protein (73 ± 2 and $82 \pm 3\%$ of the control respectively). We found that the H3 but not H_{ABC} domain is the putative active domain of Syn-1A, which bound to and inhibited the Kv2.1 channel. When co-expressed in HEK-293 cells, the open-form Syn-1A slowed down Kv2.1 channel activation ($\tau = 12.3 \pm 0.8$ ms) much more than ($P < 0.05$) WT Syn-1A ($\tau = 7.9 \pm 0.8$ ms; control $\tau = 5.5 \pm 0.6$ ms). In addition, only the open form Syn-1A, but not the WT Syn-1A, caused a significant ($P < 0.05$) left-shift in the steady-state inactivation curve ($V_{1/2} = 33.1 \pm 1.3$ and -29.4 ± 1.1 mV respectively; control $V_{1/2} = -24.8 \pm 2$ mV). The present study therefore indicates that the open form of Syn-1A is more potent than the WT Syn-1A in inhibiting the Kv2.1 channel. Such stronger inhibition by the open form of Syn-1A may limit K⁺ efflux and thus decelerate membrane repolarization during exocytosis, leading to optimization of insulin release.

Key words: channel gating, exocytosis, HEK-293 cell, Kv2.1 channel, SNARE protein, syntaxin.

INTRODUCTION

In regulated exocytosis of neurotransmitters or hormones, Ca²⁺-triggered fusion of secretory vesicles with the plasma membrane is preceded by at least two distinct steps: (1) docking of the vesicles at the plasma membrane followed by (2) priming, whereby the vesicle SNARE (soluble *N*-ethylmaleimide-sensitive fusion protein attachment protein receptor) protein synaptobrevin and two plasma-membrane target-SNARE (t-SNARE) proteins SNAP-25 (synaptosome-associated protein of 25 kD) and Syn-1A (syntaxin 1A) assemble to become a complex [1–3]. Such a complex formation pulls the vesicle and plasma membranes into very close contact, rendering the membranes ready for fusion.

When the cell is depolarized, Ca²⁺ influx through VDCC (voltage-dependent Ca²⁺ channels) is sensed by synaptotagmin causing its interaction with the t-SNARE proteins to initiate exocytosis [4,5]. This core complex formation between the SNARE proteins is prevented when Syn-1A adopts a closed form, whereby the N-terminal H_{ABC} domain of Syn-1A folds back on to the C-terminal SNARE motif (H3 domain), thus preventing the latter binding SNAP-25 and synaptobrevin [6–8]. During priming, the closed form Syn-1A opens up to form a core complex with its SNARE partners [6–8]. After exocytosis, the SNARE

complex disassembles and Syn-1A resumes its closed form. An important regulator for priming appears to be Munc-13 [5,8]. Convincing evidence for this Munc-13–syntaxin interaction in priming came from experiments employing a constitutively open mutant form of syntaxin by introducing two mutations (L165A, E166A) at the linker region between H_{ABC} and H3 [6,9]. In the *Caenorhabditis elegans unc-13* mutant, expression of the open form of syntaxin, but not the WT (wild-type) form, can rescue the nematodes from paralysis, neurotransmission defects and behavioural abnormalities [9]. Therefore the open form Syn-1A can bypass the requirement for *unc-13* in vesicle priming.

SNARE proteins are known to be tethered to various VDCCs [10,11]. This physical intimacy not only allows SNARE proteins to be immediately exposed to a high local Ca²⁺ concentration permeating through the VDCC, but also facilitates direct modulation of VDCC gating by the SNARE proteins [10–13]. Outward K⁺ currents through Kv channels (voltage-gated K⁺ channels) are responsible for repolarization, which results in the closure of VDCC and subsequently termination of exocytosis [14–16]. In HEK-293 cells (human embryonic kidney-293 cells) and *Xenopus* oocyte expression systems, we have shown in co-immunoprecipitation and electrophysiological experiments that SNARE proteins also physically and functionally interact with Kv1.1 and

Abbreviations used: GST, glutathione S-transferase; HEK-293 cells, human embryonic kidney-293 cells; Kv channel, voltage-gated K⁺ channel; SNAP-25, synaptosome-associated protein of 25 kDa; SNARE, soluble *N*-ethylmaleimide-sensitive fusion protein attachment protein receptor; t-SNARE, target SNARE; Syn-1A, syntaxin 1A; VDCC, voltage-dependent Ca²⁺ channel; WT, wild-type.

¹ Correspondence may be addressed to either of the authors (email herbert.gaisano@utoronto.ca and r.tsushima@utoronto.ca).

Kv2.1 [17–22]. Indeed we have just shown that SNARE proteins co-localize with Kv2.1 and Cav1.2 (L-type VDCC) in lipid raft domains in pancreatic β -cell plasma membrane [23], providing compelling evidence for the structural basis of the ‘excitosome’ [10,11]. Thus SNARE regulation of both the VDCC and Kv channels may help to fine-tune the excitability and exocytosis of actively secretory cells. We have previously shown that WT Syn-1A binds to the C-terminus of Kv2.1 leading to reduction in the magnitude of the Kv2.1 current and modulation of the gating properties of Kv2.1 (slowing down activation and increasing the voltage sensitivity of steady-state inactivation) [21]. We now hypothesize that the conformational changes of Syn-1A during SNARE complex assembly/disassembly in the exocytotic cycle would dynamically regulate Kv2.1 channel activities. We therefore explored the effects of the open mutant form of Syn-1A, and found that it is more potent than the WT Syn-1A in inhibiting Kv2.1 channel activities. The stronger inhibition by the open form of Syn-1A may slow down repolarization and facilitate exocytosis. We have also determined the active domain of Syn-1A for its inhibition on the Kv2.1 channel.

EXPERIMENTAL

Cell culture and transfections

HEK-293 cells were grown at 37°C in 5% CO₂ in minimal essential medium containing 1 g/l glucose, supplemented with 10% FBS (Gibco, Gaithersburg, MD, U.S.A.) and penicillin-streptomycin (100 units/ml, 100 µg/ml; Invitrogen, Burlington, ON, Canada). The cells were transiently transfected with green fluorescent protein (0.6 µg) and Kv2.1 (0.2 µg) with or without Syn-1A (1.0 µg) in 35 mm tissue culture dishes using Lipofectamine™ 2000 (Invitrogen) according to the manufacturer’s instructions. One day after transfection, cells were trypsinized, placed in 35 mm tissue culture dishes and cultured overnight before electrophysiological recordings. Transfected cells were identified by visualization of the fluorescence of the co-expressed green fluorescent protein. Only moderately green cells were chosen for experiments. For biotinylation/Western-blot experiments, to obtain a substantial amount of plasma-membrane protein, cells were grown in 100 mm tissue culture dishes and the amount of DNA used was 6 times that mentioned above for each DNA species.

DNA constructs and recombinant GST (glutathione S-transferase)-fusion proteins

The pCMV-Syn-1A (WT) was from R. Scheller (Genentech, South San Francisco, CA, U.S.A.) and pCMV-Syn-1A-L165A/E166A and pGEX-4T-1-Syn-1A L165A/E166A were from S. Sugita (Toronto Western Hospital Research Institute, Toronto, ON, Canada). The constructs pcDNA3-Kv2.1, pGEX-4T-1-Syn-1A, pGEX-5X-1-Kv2.1-N (encoding amino acids 1–183), pGEX-5X-1-Kv2.1-C1 (amino acids 412–633) and pGEX-5X-1-Kv2.1-C2 (amino acids 634–853) have been reported previously [21]. DNAs encoding Syn-1A-H_{ABC} domain (corresponding to amino acids 1–160) and Syn-1A-H₃ domain (amino acids 191–256) were generated by PCR using pCMV-Syn-1A as a template, then subcloned into pGEX-4T-1 vector (Amersham Biosciences Inc., Piscataway, NJ, U.S.A.). All constructs were verified by DNA sequencing. GST-fusion protein expression and purification were performed according to the manufacturer’s (Amersham Biosciences) instructions. Before elution of the GST-fusion protein from glutathione–agarose beads, Syn-1A protein was obtained by cleavage of GST–Syn-1A with thrombin (Sigma, St. Louis, MO, U.S.A.).

In vitro binding assays

HEK-293 cells were transfected with pcDNA3-Kv2.1, pCMV-Syn-1A (WT) or pCMV-Syn-1A-L165A/E166A using LIPOFECT-AMINE™ 2000. Two days after transfection, the HEK-293 cells were washed with ice-cold PBS (pH 7.4), then harvested in binding buffer (25 mM Hepes, pH 7.4, 100 mM KCl, 2 mM EDTA, 2% Triton X-100, 20 µM NaF, 1 mM PMSF, 1 µg/ml leupeptin and 10 µg/ml aprotinin). The cells were lysed by sonication and insoluble materials were removed by centrifugation at 25 000 g at 4°C for 30 min. For binding assay, the cell extracts were mixed with GST (negative control), GST–Kv2.1–N, GST–Kv2.1–C1, GST–Kv2.1–C2, GST–Syn-1A–H_{ABC}, GST–Syn-1A–H₃ or GST–Syn-1A–WT (all bound to glutathione agarose beads, 600 pmol protein each) and incubated at 4°C with constant agitation for 2 h. The beads were then washed three times with binding buffer. The samples were separated by SDS/PAGE (8 or 15% gel), transferred on to a nitrocellulose membrane (Millipore, Bedford, MA, U.S.A.) and identified with antibody against Syn-1A (1:2000, Sigma) or Kv2.1 (1:1000, Upstate Biotechnology, Lake Placid, NY, U.S.A.).

Electrophysiology

HEK-293 cells were voltage-clamped in the whole-cell configuration [24] using an EPC-9 amplifier and Pulse software (HEKA Elektronik, Lambrecht, Germany) as we previously described [21]. Recording pipettes were pulled from 1.5 mm borosilicate glass capillary tubes (World Precision Instruments, Sarasota, FL, U.S.A.) using a programmable micropipette puller (Sutter Instrument, Novato, CA, U.S.A.). Pipettes were then heat-polished and tip resistances ranged from 1.5 to 3 MΩ when filled with intracellular solution, containing (mM) 140 KCl, 1 MgCl₂, 1 EGTA, 10 Hepes and 5 MgATP (pH 7.25 adjusted with KOH). Bath solution contained (mM): 140 NaCl, 4 KCl, 1 MgCl₂, 2 CaCl₂, 10 Hepes (pH 7.3 adjusted with NaOH). After a whole-cell configuration was established, the cell was held at –70 mV and subjected to various experimental methods as detailed in the Results section and legends. Steady-state outward current was determined as the mean current in the final 95–99% of the pulse. All experiments were performed at room temperature (~22°C). Results obtained for the voltage dependence of activation and steady-state inactivation were fit by the Boltzmann equation: $I/I_{\max} = 1/\{1 + \exp[(V_{1/2} - V)/k]\}$ (for fitting voltage dependence of activation), or $I/I_{\max} = 1/\{1 + \exp[(V - V_{1/2})/k]\}$ (for fitting steady-state inactivation), where $V_{1/2}$ is the half-maximal activation potential (for voltage dependence of activation) or the half-maximal inactivation potential (for steady-state inactivation), and k the slope factor. Results are presented as means ± S.E.M. ANOVA was used for multiple group comparisons and statistical significance was determined by Student–Newman–Keuls test. A $P < 0.05$ was considered statistically significant.

Confocal immunofluorescence microscopy

Laser confocal immunofluorescence microscopy experiments were performed as described previously in [21]. Transfected HEK-293 cells were fixed with 100% methanol on 3-aminopropyltriethoxysilane-treated glass slides. The slides were then incubated at 4°C overnight with mouse monoclonal anti-Kv2.1 (1:100; Upstate Biotechnology) and rabbit anti-Syn-1 (1:100; Calbiochem, San Diego, CA, U.S.A.). The slides were rinsed four times in PBS containing 0.1% saponin and treated with secondary antibodies (FITC sheep anti-mouse IgG 1:500 or Texas Red-labelled goat anti-rabbit IgG 1:250) for 1 h. Next, they were incubated with 0.1% *p*-phenylenediamine (ICN, Cleveland, OH,

U.S.A.) in glycerol and examined using a laser scanning confocal imaging system (LSM-410; Carl Zeiss, Thornwood, NY, U.S.A.). FITC signal was visualized by excitation at a wavelength of 488 nm and the emitted fluorescence was measured through a 515 to 540 nm bandpass filter. Texas Red signal was visualized by an excitation wavelength of 568 nm and the emitted fluorescence was detected through a 590 nm long-pass filter.

Cell-surface biotinylation

HEK-293 cells were washed and harvested in PBS, 2 days after transfection. The cells were further washed with borate buffer (154 mM NaCl, 7.2 mM KCl, 1.8 mM CaCl₂ and 10 mM boric acid, pH 9.0) and then incubated in 5 ml of sulfo-NHS-SS-biotin (0.5 mg/ml; Pierce Biotechnology, Rockford, IL, U.S.A.) in borate buffer at 4°C for 30 min. After washing three times with ice-cold quenching buffer (192 mM glycine and 25 mM Tris, pH 8.3), cells were solubilized on ice in 500 µl of immunoprecipitation buffer (1% deoxycholic acid, 1% Triton X-100, 0.1% SDS, 150 mM NaCl, 1 mM EDTA and 10 mM Tris/HCl, pH 7.5) containing a cocktail of protease inhibitors (Roche Diagnostics, Mannheim, Germany). The cell lysate was centrifuged for 20 min at 16000 g, and the supernatant was retained. Immobilized streptavidin resin (50 µl; Pierce; 50% slurry in PBS containing 2 mM NaN₃) was added to the supernatant, which was then incubated overnight at 4°C with gentle rocking. Samples were centrifuged for 2 min at 8000 g, and the resin was washed five times with immunoprecipitation buffer. The protein was eluted from the resin by the addition of SDS/PAGE sample buffer containing 5% (w/v) 2-mercaptoethanol and incubation at 65°C for 5 min. The samples were analysed for Kv2.1 expression by Western blotting using anti-Kv2.1 (1:1000, Alomone Labs, Jerusalem, Israel). Integrated density of the bands was determined by using a commercial software (Scion Image Beta 4.02; Scion Corporation, Frederick, MA, U.S.A.).

RESULTS

Open form and WT Syn-1A decreased Kv2.1 channel surface expression and current density

As shown in Figure 1(A), substantial outward K⁺ currents were triggered by increasing depolarizing steps in HEK-293 cells transfected with Kv2.1 alone. Co-expression with WT Syn-1A or open form Syn-1A drastically decreased Kv2.1 current density (Figure 1A). The results are summarized in the I–V relationship shown in Figure 1(B). Open form Syn-1A decreased Kv2.1 current density more than WT Syn-1A as measured at +70 mV (166 ± 35 and 371 ± 93 pA/pF respectively; control = 911 ± 91 pA/pF; $P < 0.05$).

To investigate if the syntaxins decreased Kv2.1 current density by inhibiting the trafficking of Kv2.1 protein to the plasma membrane, we performed confocal immunofluorescence microscopy (Figure 2A). When Kv2.1 was expressed alone, there was bright and distinct fluorescence at the cell periphery (Figure 2A, left panel). Co-expression of WT Syn-1A resulted in a dimmer and diffused fluorescence of the Kv2.1 protein (note patches of fluorescence beneath the cell periphery; Figure 2A, middle panel), suggesting that Syn-1A (inset) may have inhibited Kv2.1 from trafficking to the plasma membrane, and a substantial proportion of Kv2.1 was retained in the cytoplasm. A similar degree of inhibition of Kv2.1 trafficking was observed with the open form Syn-1A co-expression (Figure 2A, right panel).

To determine quantitatively the amount of decrease of plasma-membrane surface expression of Kv2.1 caused by the over-

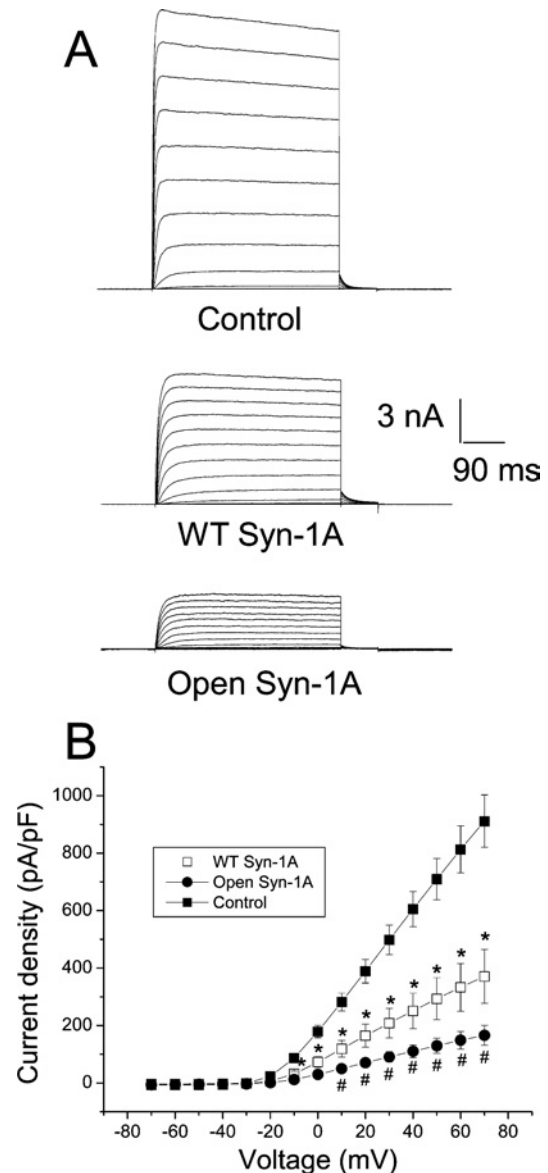


Figure 1 Open form Syn-1A decreased the current density of Kv2.1 to a greater extent than WT Syn-1A

(A) Representative traces showing outward K⁺ currents triggered by a series of pulses (from -70 to $+70$ mV, 500 ms) from a holding potential of -70 mV in HEK-293 cells expressing Kv2.1 alone, Kv2.1 with WT Syn-1A or Kv2.1 with the open form of Syn-1A. (B) Quantitative summary of (A). Currents were normalized by cell capacitance to yield the current density. Results are means \pm S.E.M. for 13–22 cells. *Significantly ($P < 0.05$) lower than control; # significantly ($P < 0.05$) lower than control and WT Syn-1A.

expression of WT and the open form Syn-1A, we performed the following study. Transfected HEK-293 cells were biotinylated so that plasma-membrane proteins can be separated using the streptavidin resin. Consistent with the results in Figure 2(A), Figure 2(B, i) shows that the level of plasma-membrane Kv2.1 protein pulled down by the streptavidin resin was decreased to a similar extent with WT and open form Syn-1A co-expression (18 ± 5 and 20 ± 12 % respectively; three separate experiments). The Kv2.1 protein content in the total lysates determined just before the treatment with streptavidin resin did not change, indicating that neither syntaxin had any significant effect on total protein synthesis of Kv2.1 (Figure 2B, ii). The greater effect of the open Syn-1A than WT Syn-1A in decreasing Kv2.1 current

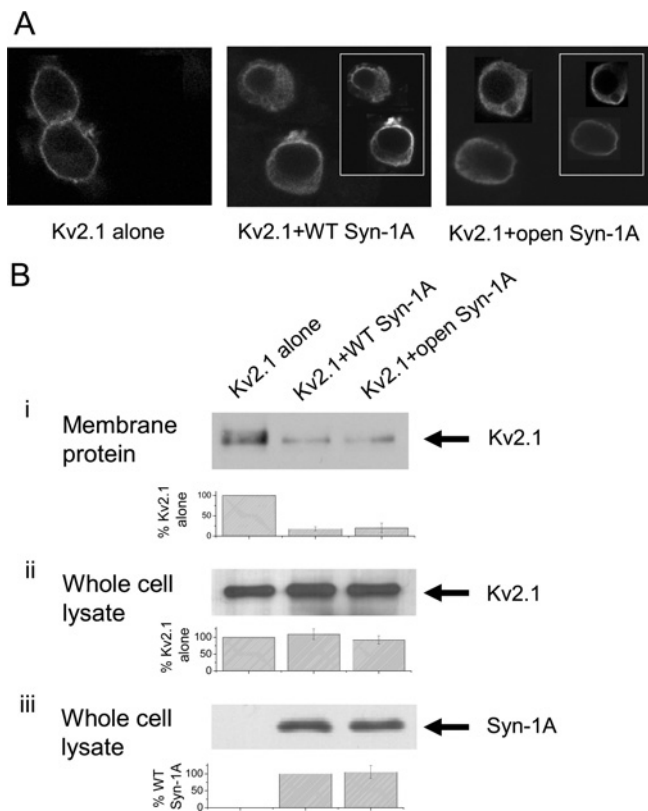


Figure 2 WT and open form Syn-1A decreased Kv2.1 channel trafficking to the plasma membrane to a similar extent

(A) Confocal microscopy showing Syn-1A inhibition of Kv2.1 surface expression. HEK-293 cells were transfected with Kv2.1 in the absence or presence of WT or open form Syn-1A. Expression of Kv2.1 alone was visualized as a bright and clear FITC fluorescence at the cell periphery (left panel). Kv2.1 fluorescence was faint and diffuse with WT or open form Syn-1A co-expression (middle and right panels). Insets show expression of syntaxins, as visualized by Texas Red fluorescence. (B) Plasma-membrane Kv2.1 protein expression. Transfected HEK-293 cells were biotinylated and solubilized as described in the Experimental section. Biotinylated proteins (plasma-membrane fraction) were isolated using the streptavidin resin. The proteins eluted from the resin (B, i) and whole cell lysates obtained before the precipitation of streptavidin (B, ii, iii) were then separated by PAGE, and Kv2.1 and Syn-1A were identified by Western blotting. The whole cell lysates are assessments of total cellular synthesis of Kv2.1 and Syn-1A. The integrated density of the bands was determined by Scion Image Beta 4.02. Results are means \pm S.E.M. for three separate experiments.

density could probably be due to a higher expression of the open Syn-1A at the plasma membrane. As Syn-1A does not possess an extracellular domain to be biotinylated, it is not possible to quantify the surface expression of Syn-1A using the biotinylation methods. However, total synthesis of both the syntaxins was similar (Figure 2B, iii). Furthermore, the surface signal for the open Syn-1A did not appear to be stronger than that for the WT Syn-1A. (insets in Figure 2A, middle and right panels).

The confocal microscopy and biotinylation/Western-blot results taken together indicate that the greater decrease in the Kv2.1 current density by the open form of Syn-1A compared with the WT Syn-1A, was probably not due to a more severe defect in trafficking, but rather due to a direct and more potent inhibition by the open form of Syn-1A on Kv2.1 channel gating.

Direct inhibition of Kv2.1 channel activity by the open form of Syn-1A is greater than that by WT Syn-1A

We had shown that WT-Syn-1A binds strongly to the Kv2.1-C1 (amino acids 412–633) and Kv2.1-C2 termini (amino acids 634–

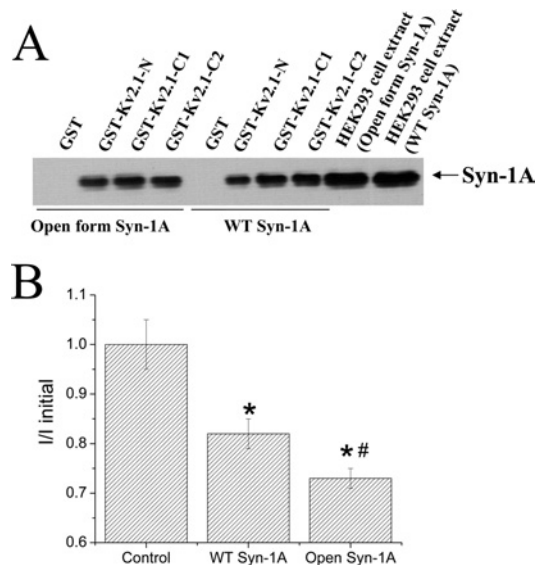


Figure 3 Direct inhibition of Kv2.1 channel activity by open form Syn-1A is greater than that by WT Syn-1A

(A) Open form Syn-1A, like WT Syn-1A, binds to Kv2.1 N- and C-termini. HEK-293 cells were transfected with WT Syn-1A or open form Syn-1A. The cell extracts were incubated with GST (as a negative control), GST-Kv2.1-N, -C1 or -C2 domain proteins (all bound to glutathione agarose beads) as described in the Experimental section. The Syn-1A proteins pulled down by these Kv2.1 domain proteins were separated by SDS/PAGE (15% gel) and identified by Western blotting. The two lanes on the far right represent cell extracts not incubated with GST-Kv2.1 domain proteins. Results shown are representative of four separate experiments. (B) The effects of dialysis of GST, WT Syn-1A or open form Syn-1A (all at 300 nM) on Kv2.1 current magnitude were tested by giving +70 mV pulses (250 ms) from a holding potential of -70 mV after membrane break-in. Currents were measured 5 min after break-in, and normalized to the initial current magnitude immediately after membrane rupture. Results are means \pm S.E.M. for 8–15 cells. *, Significantly lower ($P < 0.05$) than GST control; #, significantly lower ($P < 0.05$) than GST control and WT Syn-1A.

853) but less strongly to Kv2.1-N terminus (amino acids 1–182) [21]. In the present study, we confirm that the open form of Syn-1A also binds to these Kv2.1 domains. As shown in Figure 3(A), GST-Kv2.1-N, -C1 and -C2 domain proteins (all bound to glutathione beads) were able to pull down similar amounts of the open form of Syn-1A when compared with WT Syn-1A. GST, as a negative control, did not bind either the open form or WT Syn-1A.

We then compared the direct and functional effects of these Syn-1A proteins on Kv2.1 by dialysing recombinant GST-Syn-1A proteins into Kv2.1-transfected cells (Figure 3B). Dialysis of the control GST protein did not significantly affect the current magnitude. Dialysis of GST-Syn-1A WT into the cell for 5 min caused a small ($18 \pm 3\%$) but significant ($P < 0.05$) decrease in the magnitude of current. The decrease in the magnitude of the current by dialysis of the open form Syn-1A was greater ($27 \pm 2\%$) and significantly different from WT Syn-1A ($P < 0.05$), providing evidence for a stronger direct inhibition of Kv2.1 by the open form of Syn-1A.

Putative domain within Syn-1A that inhibits Kv2.1

The greater inhibition by the open form of Syn-1A prompted us to examine which Syn-1A domain(s) might be mediating the inhibition on Kv2.1. In its closed form, Syn-1A N-terminal H_{ABC} flips over on to the C-terminal H3 domain like a hairpin, blocking H3 domain binding to a number of Syn-1A interacting proteins [6]. When Syn-1A is activated to its open form, Syn-1A straightens out to expose fully the H_{ABC} and H3 domains [6]. The

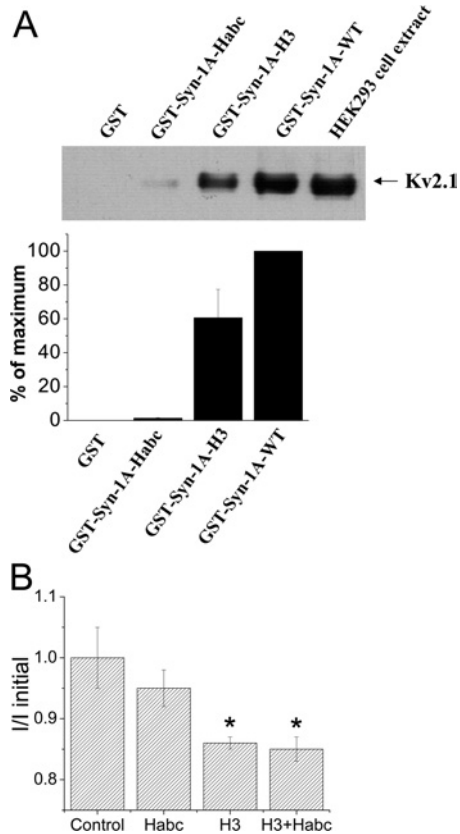


Figure 4 The H3 domain is the putative Syn-1A domain which binds and inhibits Kv2.1

(A) H3 domain, but not H_{ABC} domain, of Syn-1A binds to Kv2.1. GST, GST-Syn-1A-WT, GST-Syn-1A-H_{ABC} or -H3 (all bound to glutathione agarose beads) were incubated with Kv2.1-overexpressing HEK-293 cell extracts as described in the Experimental section. The Kv2.1 protein pulled down by these Syn-1A domain proteins was then identified by Western blotting. The top panel shows a representative blot of three separate experiments. The lane on the far right represents cell extract not incubated with GST-Syn-1A domain proteins. Lower panel: a summary of three experiments (means \pm S.E.M.). The integrated density of the bands was determined by Scion Image Beta 4.02. (B) The effects of dialysis of GST, H3, H_{ABC} or a combination of H3 and H_{ABC} (all at 300 nM) on Kv2.1 current magnitude, 5 min after membrane break-in. Methods were the same as in Figure 3(B). Results are means \pm S.E.M. for 6–13 cells. *, Both the H3 and H3 + H_{ABC} combination significantly ($P < 0.05$) decreased the current magnitude of Kv2.1.

H3 domain has been shown to be the active domain of Syn-1A that causes inhibition of N-type VDCC and epithelial Na⁺ channels [25,26].

We therefore examined next which of these Syn-1A domains might be the putative domain that binds and modulates Kv2.1. We used GST-Syn-1A-H3 and GST-Syn-1A-H_{ABC} (bound to glutathione agarose beads) to pull down Kv2.1 from Kv2.1-overexpressing HEK-293 cell extract (Figure 4A). GST-Syn-1A-H_{ABC} bound very weakly to Kv2.1. In contrast, GST-Syn-1A-H3 domain bound strongly to Kv2.1, but the binding was less than GST-Syn-1A-WT. GST alone did not bind Kv2.1 at all. Consistently, dialysis of the recombinant H3 domain into Kv2.1-expressing cells (Figure 4B) significantly inhibited the Kv2.1 current ($14 \pm 2\%$, $P < 0.05$). The inhibitory effect of the H_{ABC} domain was very small and insignificant. Interestingly, the addition of H_{ABC} to H3 did not reverse H3-mediated inhibition of Kv2.1, and in fact the effect on Kv2.1 was not different from H3 alone. The latter result suggests that the distinct effects of the open and closed forms of Syn-1A on Kv2.1 are not simply conferred by the

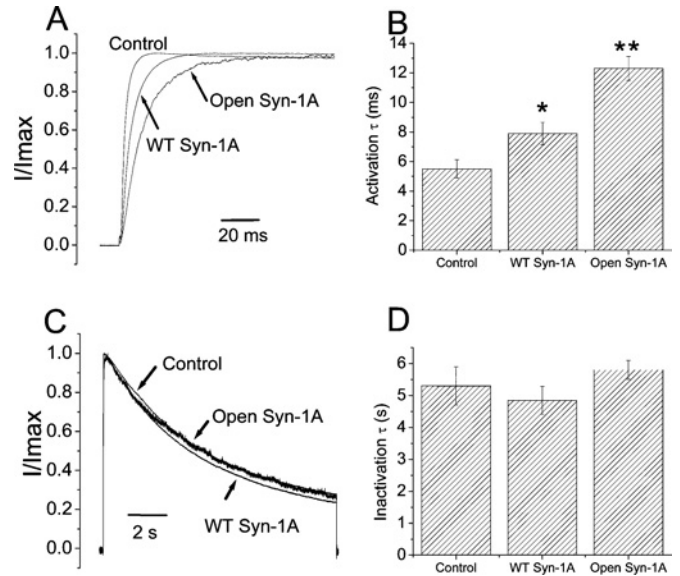


Figure 5 Open form of Syn-1A slowed down Kv2.1 current activation more than WT Syn-1A

(A) Outward K⁺ currents were triggered by a +70 mV pulse (250 ms) from a holding potential of -70 mV in HEK-293 cells expressing Kv2.1 with or without syntaxins. Currents shown are normalized to its peak magnitude and overlapped for comparison. Activation time constants are obtained by an exponential fit to the rising phase of the current and are summarized in (B). Results are means \pm S.E.M. for 13–18 cells. *, Significantly different ($P < 0.05$) from control (Kv2.1 alone); and **, significantly different ($P < 0.05$) from control and WT Syn-1A. (C) To show inactivation, outward K⁺ currents were triggered by a prolonged +70 mV pulse (12 s) from a holding potential of -70 mV in HEK-293 cells expressing Kv2.1 with or without syntaxins. Currents shown are normalized to its peak magnitude and overlapped for comparison. Inactivation time constants are obtained by an exponential fit to the decaying phase of the current, and are summarized in (D). Results are means \pm S.E.M. for 7–8 cells. Neither WT nor open form Syn-1A affected the rate of inactivation.

independent actions of its H3 and H_{ABC} domains, but also by the conformations adopted by the full-length Syn-1A proteins.

Open Syn-1A modulation of Kv2.1 channel gating is distinct from that by WT Syn-1A

We previously reported that WT Syn-1A profoundly affected Kv2.1 channel gating properties, including the rate of activation and voltage dependence of steady-state inactivation. We next explored whether the open form Syn-1A differed from the WT Syn-1A in modulating these channel-gating properties. As both syntaxins decreased current density, only those cells expressing currents ≥ 4 nA were selected for analysis because HEK-293 cells express endogenous outward K⁺ currents approx. 0.4 nA in amplitude (results not shown). Kv2.1 had a rapid activation rate, with a τ of 5.5 ± 0.6 ms (Figures 5A and 5B). Overexpressed WT Syn-1A significantly slowed down the activation rate ($\tau = 7.9 \pm 0.8$ ms; $P < 0.05$). The open form Syn-1A slowed down activation more than WT Syn-1A ($\tau = 12.3 \pm 0.8$ ms; $P < 0.05$). Kv2.1 exhibited a very slow inactivation rate, which was not affected by the WT or open form of Syn-1A (Figures 5C and 5D).

Since both syntaxins slowed down Kv2.1 activation, we then investigated if they would affect the voltage dependence of activation of Kv2.1. To study this, instantaneous activation curves were obtained using the method in which voltage steps from -50 to +60 mV in 10 mV increments were followed by tail currents elicited at -40 mV. Normalized peak tail currents were then plotted against the various voltage steps and fitted to the Boltzmann equation (Figure 6A). Surprisingly, neither syntaxin

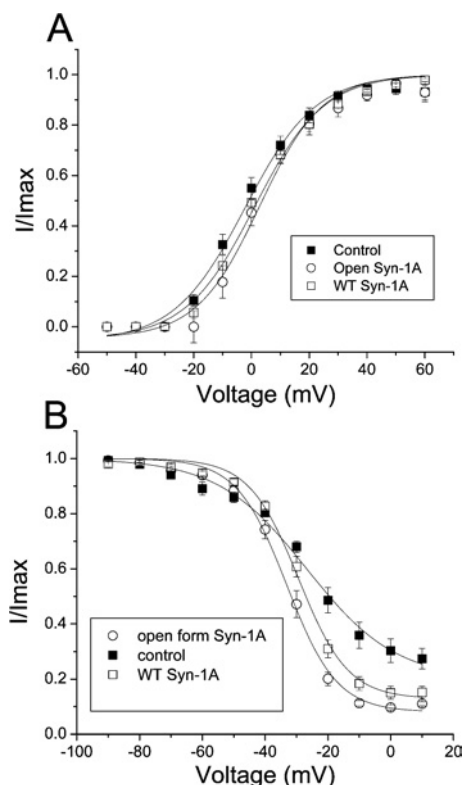


Figure 6 Open form Syn-1A caused a left-shift in the steady-state inactivation curve of Kv2.1 but had no effect on the voltage dependence of activation

(A) Instantaneous activation curves. Voltage steps from -50 to $+60$ mV (500 ms) delivered in 10 mV increments from a holding potential of -70 mV were followed by a -40 mV step to trigger tail currents. Normalized peak tail currents are then plotted against the various voltage steps. The curves are best fit by the Boltzmann equation. Neither WT nor the open form of Syn-1A significantly affected the voltage dependence of activation. Results are means \pm S.E.M. for 7–10 cells. (B) Steady-state inactivation experiments. A dual-pulse method was used in which a test pulse step of $+70$ mV was preceded by a long pre-pulse (12 s) of different potentials. The test pulse currents are normalized to the largest test pulse current and plotted against the pre-pulse voltages. The curves are best fit by the Boltzmann equation. Both syntaxins significantly decreased the slope factors while only open form Syn-1A caused a significant left-shift in $V_{1/2}$ (see the Results section for details). Results are means \pm S.E.M. for 7–8 cells.

significantly altered the voltage dependence of the activation of Kv2.1.

We next performed steady-state inactivation experiments to determine channel availability as a function of the membrane potential. A dual-pulse method was used in which a test pulse step of $+70$ mV was preceded by a long pre-pulse (12 s) to different potentials. The test pulse currents were normalized to the largest test pulse current and plotted against the pre-pulse voltages. The results were best fit with the Boltzmann equation (Figure 6B). Kv2.1 currents have a half-maximal inactivation potential ($V_{1/2}$) of -24.8 ± 2.0 mV. Consistent with our previous report [21], the modest leftward shift of the inactivation curve ($V_{1/2}$ value of -29.4 ± 1.1 mV) caused by WT Syn-1A was statistically insignificant. In contrast, open Syn-1A caused a larger hyperpolarizing shift in the inactivation curve than WT Syn-1A ($V_{1/2}$ value of -33.1 ± 1.3 mV). This $V_{1/2}$ value is significantly different ($P < 0.05$) from those of control and WT Syn-1A. WT Syn-1A significantly decreased the slope factor from 15.2 ± 2.1 to 7.6 ± 0.4 ($P < 0.05$), indicating that WT Syn-1A increased the sensitivity of voltage-dependent inactivation within the physiological range (-40 to -10 mV). Open Syn-1A also significantly

($P < 0.05$) decreased the slope factor (7.8 ± 0.6), but this value was similar to that caused by the WT Syn-1A.

DISCUSSION

Open form Syn-1A is a stronger inhibitor of Kv2.1 currents compared with the WT Syn-1A

In our recent report, we showed that WT Syn-1A inhibits the magnitude of the Kv2.1 current and modulates its gating properties by binding to the cytoplasmic C-terminus of Kv2.1 channel [21]. During exocytosis, Syn-1A converts from the closed state to an open state, particularly during the process of priming [1–8]. We therefore examined in the present work if the open and closed forms of Syn-1A differentially modulate the gating properties of Kv2.1. In our previous works showing Syn-1A regulation of Kv channels and VDCC, the form of Syn-1A used was the WT [12,19–22]. Of note, the WT Syn-1A may not entirely represent the closed form, as it was recently shown by single-molecule fluorescence resonance energy transfer measurement to exhibit a rapid dynamic equilibrium between the closed and open forms [27]. Therefore to examine the specific actions of the activated open form Syn-1A, we employed the mutant Syn-1A which is constitutively open by the introduction of two mutations at the linker region (L165A, E166A) [6,9].

In co-expression experiments, the open form of Syn-1A decreased the Kv2.1 current density more effectively than WT Syn-1A. This does not appear to result from stronger inhibition of trafficking of Kv2.1 to the cell surface, as confocal microscopy and biotinylation results showed that the open form and WT Syn-1A inhibited Kv2.1 plasma-membrane surface expression to a similar extent. The stronger channel inhibition by the open form Syn-1A compared with WT Syn-1A may be contributed by possible higher expression levels of the open form Syn-1A. However, our results from confocal microscopy and Western-blot analysis do not support this possibility. Another point to argue against this possibility is that in our previous work [21], we had shown that an even higher expression of WT Syn-1A compared with the results reported in the present study did not achieve the degree of gating modulation observed with the open form of Syn-1A (see below). Taken together, the results suggest that the open form of Syn-1A causes a stronger direct inhibition on Kv2.1 compared with WT Syn-1A.

To verify further that the open form of Syn-1A is more potent compared with WT Syn-1A, recombinant proteins of the open form or WT Syn-1A were dialysed into Kv2.1-expressing cells. The results indicate that the open form Syn-1A is indeed stronger than WT Syn-1A in directly inhibiting the channel. As the H3 domain is fully exposed after Syn-1A opens up, we tested whether the H3 domain would act similarly to the open form of Syn-1A. H3 has been shown to be the active domain in mediating Syn-1A inhibition of N-type VDCC and the epithelial Na^+ channel [25,26]. Indeed, H3 but not H_{ABC} caused a significant inhibition of the Kv2.1 channel activities. Consistently, H3 bound Kv2.1 strongly, whereas H_{ABC} exhibited almost no binding to Kv2.1. However, H3 inhibition ($14 \pm 2\%$) was significantly less ($P < 0.05$) than that by the open form of Syn-1A ($27 \pm 2\%$), and the addition of the 'negative' regulatory H_{ABC} domain did not enhance or prevent the inhibiting action of the H3 domain. These results suggest that optimal inhibition of the Kv2.1 channel may require either the full-length Syn-1A molecule or a distinct conformational change to the H3 domain when Syn-1A assumes the open conformation. In contrast, Jarvis et al. [28] reported that the very N-terminus including the H_{A} domain appeared to be sufficient to bind and anchor to the synprint site of N-type

VDCC. Although the open form of Syn-1A inhibited Kv2.1 more than WT Syn-1A, it bound to Kv2.1 channel termini only as efficiently as WT Syn-1A. It may be possible that the open form of Syn-1A could bind to some other domains of Kv2.1 that WT Syn-1A did not bind to, or the open form Syn-1A may form distinct complexes with these Kv2.1 domains. Our initial reported results [21] showed that, while Syn-1A (WT) also binds the Kv2.1 cytoplasmic N-terminus (as confirmed in Figure 3A), the channel inhibition did not seem to be transduced via this channel domain.

Open form of Syn-1A is a stronger inhibitor than WT Syn-1A in modulating Kv2.1 gating

Syn-1A is a plasma membrane-bound protein, with the last 22 amino acids at the C-terminus inserted into the plasma membrane, and the rest of the protein free in the cytoplasm [25]. The GST-fusion proteins of Syn-1A (or its domains) lack the transmembrane domain, and therefore, their ability to inhibit directly Kv2.1 suggests that neither the membrane spanning domain of Syn-1A nor its anchoring to the plasma membrane is absolutely required for Kv2.1 inhibition. Nevertheless, the relatively small inhibition on Kv2.1 by dialysed syntaxins may be due to sub-optimal targeting to the plasma membrane. We therefore co-expressed Kv2.1 and syntaxins in subsequent experiments to examine the effects of the WT and the open form of Syn-1A on Kv2.1 gating. We previously showed that overexpressed WT Syn-1A slows down activation and increases the voltage sensitivity of steady-state inactivation of Kv2.1 ([21]; also see Figures 5 and 6). When we used dialysed WT-Syn-1A, we did not notice this slowing down of activation (results not shown), suggesting that membrane targeting or the membrane-spanning domain of Syn-1A might support the modulation of Kv2.1 gating. In the present study, we further report much stronger inhibitory effects with the open form of Syn-1A overexpression. First, the open form of Syn-1A slows down the time constant of Kv2.1 activation from 5.5 to 12.3 ms, much longer than the 7.9 ms observed with WT Syn-1A. Secondly, although both syntaxins increased the voltage sensitivity of steady-state inactivation, only the open form of Syn-1A caused a significant leftward shift in the inactivation of $V_{1/2}$ (8.3 mV compared with 4.6 mV by WT Syn-1A). In our previous work [21], increasing the dosage of WT Syn-1A cDNA used in the transfection to 3 μ g (from 1 μ g) decreased Kv2.1 current density further to approx. 20% of control (similar to that observed in the present study with 1 μ g of open form Syn-1A; see Figure 1), but did not cause any significantly stronger effects on Kv2.1 gating (activation τ slowed down to only 8.5 ms and leftward shift in inactivation $V_{1/2}$ was only 4.8 mV). These observations suggest that the stronger effects of open form Syn-1A on Kv2.1 gating compared with WT Syn-1A are unlikely to be the result of higher expression of open form Syn-1A, but rather because of the qualitative differences between the two forms of syntaxins on Kv2.1 gating.

Physiological significance

We have provided here the first report showing that open form Syn-1A inhibits the Kv2.1 channel more than WT Syn-1A. We have also identified the structural determinant of Syn-1A (H3 domain) in mediating Kv2.1 inhibition. Since WT Syn-1A has been shown to 'flip-flop' between the closed and open forms [27], our previous report using WT Syn-1A [21] may not entirely represent the closed form. It therefore becomes reasonable to speculate that the closed form may inhibit Kv2.1 less than WT Syn-1A. Unfortunately, there is so far no constitutively closed form Syn-1A reported to verify this point. Interestingly, Zamponi's group has demonstrated that while both WT and open form Syn-1A equally

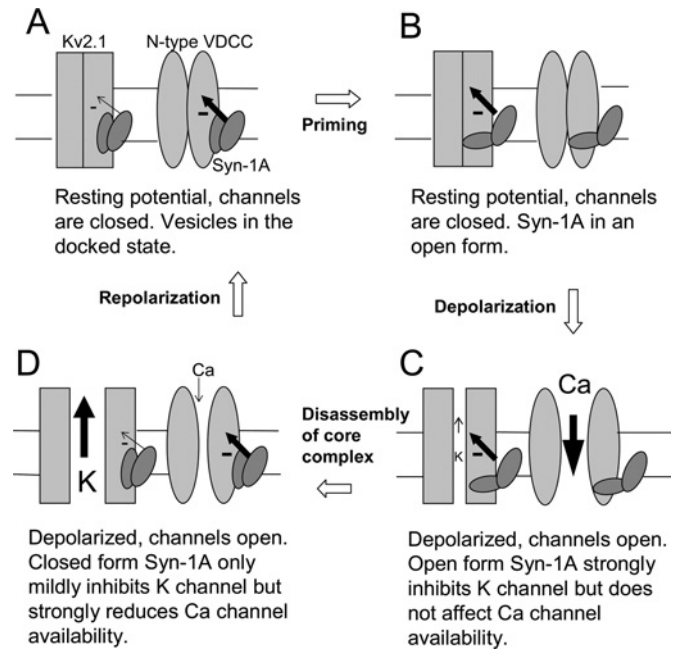


Figure 7 A schematic diagram to illustrate how the conformational changes of Syn-1A might affect Kv2.1 and N-type VDCC gating during the exocytotic cycle

The size of the minus signs and the arrows accompanying the minus signs indicates the relative strength of channel inhibition. SNAP-25 and synaptobrevin are omitted for clarity. **(A)** Before priming, the cell is at rest, channels are closed and Syn-1A is in the closed conformation. **(B)** After priming, the cell is still at rest, channels are closed but Syn-1A has already opened up. **(C)** Depolarization opens both the Kv2.1 channel and N-type VDCC. Kv2.1 is strongly inhibited by the open form of Syn-1A with limited K^+ efflux (small arrow through the channel pore). N-type VDCC availability is not affected by the open form Syn-1A, resulting in substantial Ca^{2+} influx (big arrow through the channel pore). **(D)** After exocytosis, core complex disassembles and Syn-1A resumes the closed configuration, resulting in decreased N-type VDCC availability. The closed form Syn-1A exerts less inhibition on Kv2.1 channel and the subsequent larger K^+ efflux accelerates repolarization. See text for a more detailed discussion.

support G-protein inhibition of N-type VDCC, the availability of N-type VDCC was only decreased by WT Syn-1A, but not by the open form Syn-1A [28]. What is the physiological significance of such reciprocal modulation of VDCC and Kv channels by the conformational changes of Syn-1A? The model depicted in Figure 7, which takes into consideration of our results and the interpretation by Zamponi's group [28], proposes that such reciprocal modulation optimally regulates the membrane potential and thus exocytosis. When the vesicles are just docked and the cell is at rest, Syn-1A is in the closed form (Figure 7A). The closed form Syn-1A decreases significantly the availability of N-type VDCC but causes little inhibition on Kv2.1. After priming, Syn-1A adopts an open configuration and causes stronger inhibition on Kv2.1 but has no inhibitory effect on N-type VDCC (Figure 7B). Since Kv2.1 channel and N-type VDCC are still closed at this stage, the inhibition by either the closed or open form of Syn-1A does not bear much significant effects. As the cell is stimulated and depolarized, both Kv2.1 and N-type VDCC open (Figure 7C). Since the open form of Syn-1A does not decrease N-type VDCC availability, it allows maximal Ca^{2+} influx. At the same time, the open form of Syn-1A strongly inhibits Kv2.1 to limit K^+ efflux, thus decelerating membrane repolarization and consequently augmenting Ca^{2+} influx during exocytosis. After exocytosis, as the SNARE core complex disassembles, Syn-1A reverts back to the closed form (Figure 7D). The closed form Syn-1A strongly decreases N-type VDCC availability, resulting in a diminished

Ca²⁺ influx. At the same time, the closed form Syn-1A exerts less inhibition on Kv2.1, allowing more K⁺ efflux and accelerating repolarization. Eventually, the cell repolarizes to its resting potential with the consequent closure of both the N-type VDCC and Kv2.1. Further studies are necessary to determine whether other types of VDCC, other Kv family members and K_{ATP} channels [29,30] are also differentially modulated by the conformational changes of Syn-1A.

This work was supported by grants to H.Y.G. from the Canadian Institutes of Health Research (MOP-64465), Canadian Diabetes Association (1209) and the Juvenile Diabetes Research Foundation (1-2001-521) and by grants to R.G.T. from the J.H. Cummings Foundation, J.P. Bickell Foundation and the Heart and Stroke Foundation of Ontario (NA 5012; to R.G.T. and H.Y.G.). R.G.T. is supported by a New Investigator Award from the Heart and Stroke Foundation of Canada. Y.M.L. was supported by Fellowship Awards from the Department of Medicine (University of Toronto) and Canadian Diabetes Association in honour of the late Evelyn J. Parker.

REFERENCES

- Gerber, S. H. and Sudhof, T. C. (2002) Molecular determinants of regulated exocytosis. *Diabetes* **51** (Suppl. 1), S3–S11
- Rizo, J. and Sudhof, T. C. (2002) Snares and Munc18 in synaptic vesicle fusion. *Nat. Rev. Neurosci.* **3**, 641–653
- Rettig, J. and Neher, E. (2002) Emerging roles of presynaptic proteins in Ca²⁺-triggered exocytosis. *Science* **298**, 781–785
- Brunger, A. T. (2000) Structural insights into the molecular mechanism of Ca²⁺-dependent exocytosis. *Curr. Opin. Neurobiol.* **10**, 293–302
- Li, L. and Chin, L. S. (2003) The molecular machinery of synaptic vesicle exocytosis. *Cell Mol. Life. Sci.* **60**, 942–960
- Dulubova, I., Sugita, S., Hill, S., Hosaka, M., Fernandez, I., Sudhof, T. C. and Rizo, J. (1999) A conformational switch in syntaxin during exocytosis: role of munc18. *EMBO J.* **18**, 4372–4382
- Yang, B., Steegmaier, M., Gonzalez, Jr, L. C. and Scheller, R. H. (2000) nSec1 binds a closed conformation of syntaxin1A. *J. Cell Biol.* **148**, 247–252
- Brose, N., Rosenmund, C. and Rettig, J. (2000) Regulation of transmitter release by Unc-13 and its homologues. *Curr. Opin. Neurobiol.* **10**, 303–311
- Richmond, J. E., Weimer, R. M. and Jorgensen, E. M. (2001) An open form of syntaxin bypasses the requirement for UNC-13 in vesicle priming. *Nature (London)* **412**, 338–341
- Catterall, W. A. (1999) Interactions of presynaptic Ca²⁺ channels and snare proteins in neurotransmitter release. *Ann. N.Y. Acad. Sci.* **868**, 144–159
- Atlas, D. (2001) Functional and physical coupling of voltage-sensitive calcium channels with exocytotic proteins: ramifications for the secretion mechanism. *J. Neurochem.* **77**, 972–985
- Kang, Y., Huang, X., Pasyk, E. A., Ji, J., Holz, G. G., Wheeler, M. B., Tsushima, R. G. and Gaisano, H. Y. (2002) Syntaxin-3 and syntaxin-1A inhibit L-type calcium channel activity, insulin biosynthesis and exocytosis in beta-cell lines. *Diabetologia* **45**, 231–241
- Ji, J., Yang, S. N., Huang, X., Li, X., Sheu, L., Diamant, N., Berggren, P. O. and Gaisano, H. Y. (2002) Modulation of L-type Ca²⁺ channels by distinct domains within SNAP-25. *Diabetes* **51**, 1425–1436
- Hille, B. (1992) *Ionic Channels in Excitable Membranes*, 2nd edn, pp. 119–135. Sinauer Associates., Sunderland, MA
- Nichols, C. G. and Koster, J. C. (2002) Diabetes and insulin secretion: whither KATP? *Am. J. Physiol. Endocrinol. Metab.* **283**, E403–E412
- Yellen, G. (2002) The voltage-gated potassium channels and their relatives. *Nature (London)* **419**, 35–42
- Ji, J., Tsuk, S., Salapatek, A. M., Huang, X., Chikvashvili, D., Pasyk, E. A., Kang, Y., Sheu, L., Tsushima, R., Diamant, N. et al. (2002) The 25-kDa synaptosome-associated protein (SNAP-25) binds and inhibits delayed rectifier potassium channels in secretory cells. *J. Biol. Chem.* **277**, 20195–20204
- MacDonald, P. E., Wang, G., Tsuk, S., Dodo, C., Kang, Y., Tang, L., Wheeler, M. B., Cattral, M. S., Lakey, J. R., Salapatek, A. M. et al. (2002) Synaptosome-associated protein of 25 kilodaltons modulates Kv2.1 voltage-dependent K(+) channels in neuroendocrine islet beta-cells through an interaction with the channel N terminus. *Mol. Endocrinol.* **16**, 2452–2461
- Fili, O., Michaelievski, I., Bledi, Y., Chikvashvili, D., Singer-Lahat, D., Boshwitz, H., Linal, M. and Lotan, I. (2001) Direct interaction of a brain voltage-gated K+ channel with syntaxin 1A: functional impact on channel gating. *J. Neurosci.* **21**, 1964–1974
- Michaelievski, I., Chikvashvili, D., Tsuk, S., Fili, O., Lohse, M. J., Singer-Lahat, D. and Lotan, I. (2002) Modulation of a brain voltage-gated K+ channel by syntaxin 1A requires the physical interaction of Gbetagamma with the channel. *J. Biol. Chem.* **277**, 34909–34917
- Leung, Y. M., Kang, Y., Gao, X., Xia, F., Xie, H., Sheu, L., Tsuk, S., Lotan, I., Tsushima, R. G. and Gaisano, H. Y. (2003) Syntaxin 1A binds to the cytoplasmic C terminus of Kv2.1 to regulate channel gating and trafficking. *J. Biol. Chem.* **278**, 17532–17538
- Michaelievski, I., Chikvashvili, D., Tsuk, S., Singer-Lahat, D., Kang, Y., Linal, M., Gaisano, H. Y., Fili, O. and Lotan, I. (2003) Direct interaction of target SNAREs with the Kv2.1 channel. Modal regulation of channel activation and inactivation gating. *J. Biol. Chem.* **278**, 34320–34330
- Xia, F., Gao, X., Kwan, E., Lam, P. P., Chan, L., Sy, K., Sheu, L., Wheeler, M. B., Gaisano, H. Y. and Tsushima, R. G. (2004) Disruption of pancreatic beta-cell lipid rafts modifies Kv2.1 channel gating and insulin exocytosis. *J. Biol. Chem.* **279**, 24685–24691
- Hamill, O. P., Marty, A., Neher, E., Sakmann, B. and Sigworth, F. J. (1981) Improved patch-clamp techniques for high-resolution current recording from cells and cell-free membrane patches. *Pflügers Arch.* **391**, 85–100
- Bezprozvanny, I., Zhong, P., Scheller, R. H. and Tsien, R. W. (2000) Molecular determinants of the functional interaction between syntaxin and N-type Ca²⁺ channel gating. *Proc. Natl. Acad. Sci. U.S.A.* **97**, 13943–13948
- Condliffe, S. B., Carattino, M. D., Frizzell, R. A. and Zhang, H. (2003) Syntaxin 1A regulates ENaC via domain-specific interactions. *J. Biol. Chem.* **278**, 12796–12804
- Margittai, M., Widengren, J., Schweinberger, E., Schroder, G. F., Felekyan, S., Hausteiner, E., Konig, M., Fasshauer, D., Grubmüller, H., Jahn, R. et al. (2003) Single-molecule fluorescence resonance energy transfer reveals a dynamic equilibrium between closed and open conformations of syntaxin 1. *Proc. Natl. Acad. Sci. U.S.A.* **100**, 15516–15521
- Jarvis, S. E., Barr, W., Feng, Z. P., Hamid, J. and Zamponi, G. W. (2002) Molecular determinants of syntaxin 1 modulation of N-type calcium channels. *J. Biol. Chem.* **277**, 44399–44407
- Pasyk, E., Kang, Y., Huang, X., Cui, N., Sheu, L. and Gaisano, H. Y. (2004) Syntaxin-1A binds the nucleotide-binding folds of sulphonylurea receptor 1 to regulate the K_{ATP} channel. *J. Biol. Chem.* **279**, 4234–4240
- Cui, N., Kang, Y., He, Y., Leung, Y. M., Xie, H., Pasyk, E., Gao, X., Sheu, L., Hansen, J. B., Wahl, P. et al. (2004) H3 domain of syntaxin-1A inhibits K_{ATP} channels by its actions on the sulphonylurea receptor 1 nucleotide-binding folds-1 and -2. *J. Biol. Chem.* **279**, 53259–53265

Received 22 September 2004/27 October 2004; accepted 1 November 2004

Published as BJ Immediate Publication 1 November 2004, DOI 10.1042/BJ20041625